



HAL
open science

Trajectory-Based Synthesis of Propulsion Systems for Fixed-Thrusters AUVs

Olivier Chocron, Emmanuel Delaleau

► **To cite this version:**

Olivier Chocron, Emmanuel Delaleau. Trajectory-Based Synthesis of Propulsion Systems for Fixed-Thrusters AUVs. 22nd CISM IFToMM Symposium on Robot Design, Dynamics and Control (ROMANSY 2018), Jun 2018, Rennes, France. pp.380-381, 10.1007/978-3-319-78963-7_48. hal-01823105v1

HAL Id: hal-01823105

<https://hal.science/hal-01823105v1>

Submitted on 25 Jun 2018 (v1), last revised 17 Jul 2018 (v2)

HAL is a multi-disciplinary open access archive for the deposit and dissemination of scientific research documents, whether they are published or not. The documents may come from teaching and research institutions in France or abroad, or from public or private research centers.

L'archive ouverte pluridisciplinaire **HAL**, est destinée au dépôt et à la diffusion de documents scientifiques de niveau recherche, publiés ou non, émanant des établissements d'enseignement et de recherche français ou étrangers, des laboratoires publics ou privés.

Trajectory-Based Synthesis of Propulsion Systems for Fixed-Thrusters AUVs

Olivier Chocron^{1,3} and Emmanuel Delaleau^{2,3}

¹ Institut de Recherche Dupuy de Lôme, CNRS UMR 6027. chocron@enib.fr

² Department of Mechatronics. delaleau@enib.fr

³ École nationale d'ingénieurs de Brest, Technopôle Brest-Iroise,
CS 73862, 29 238 Brest, France

Abstract. This paper presents a synthesis method for the Autonomous Underwater Vehicle (AUV) propulsion system based on the features of a trajectory to follow. This method is based on solid/fluid dynamics analysis of a AUV performing the trajectory following task and gives actuation requirements to achieve it properly. This actuation is then used to generate a propulsion system under the form of a Thrust Configuration Matrix (TCM) that is compatible with the desired trajectory. From this matrix the number of thrusters, their position and direction can then be extracted to synthesis a fitted propulsion system. Thus, the propulsion capabilities of the robot will match the trajectory characteristics and it will be able to follow it. The objective of this work is to provide an evaluation as well as a design method to produce a controllable AUV for a given task. A second use of such an analysis is to provide an evaluation process allowing to perform AUV task-based design. The method is developed for generic fixed-thrusters AUVs on any trajectory, and is applied to an existing 4-thrusters AUV for a seabed scanning flat trajectory. The method shows why the initial AUV propulsion does not match the task and what is the solution solving the issue.

Keywords: AUV, Propulsion synthesis, Fixed-Thruster.

1 Introduction

Thanks to its autonomy, nowadays Underwater Autonomous Vehicles (AUVs) can perform long range surveillance missions and deep sea operations. This kind of vehicles are also used in off-shore installations, to map the sea floor, to secure harbors, to search for sea-mines, among other activities [1]. With enough effort in research, AUVs capabilities will be expanded allowing them to perform even more demanding tasks than the ones accomplished nowadays. Precisely, most AUVs are designed for specific applications as shown in [14]. In a long range type AUV, attention is focused on reducing drag forces and increasing thruster efficiency in order to reduce energy consumption and provide the AUV with more autonomy. Usually under-actuated, this type of vehicles are commonly propelled by a rear thruster and steered by control surfaces. The hull has a hydrodynamic

design in order to reduce drag forces and to improve the autonomy capabilities of the AUV. Fully maneuverable AUVs have at least as many thrusters as their operational space has degrees of freedom (DOF), usually six. Their design is focused on improving agility and multi-directional response (holonomy), which makes these vehicles energy-intensive ([16]).

Regarding the propulsion system, several architectures have been proposed. We can divide them into three categories: classical rear propeller and control surface architectures [23], bio-mimetic propulsion [25, 26, 8] and vector thrust [3]. The latter can be achieved by different means: Some authors use a steerable rear propeller for propulsion, maneuvering and control [2, 17, 18, 10, 9, 13]. Some others make collective and cyclic pitch propellers by using a swash plate [12] or by using shape-memory alloys [24]. Vector propulsion can be achieved by adding forces from fixed thrusters [19, 20] or using re-orientable (or reconfigurable) propellers [11, 4, 22]. Using vector thrusters, it has been shown that a dynamic reconfiguration of the propulsion would allow to adapt the AUV to different in-mission tasks specifications [5]. Meanwhile, finding the fitted propulsion configuration for a given task remain a challenge.

This work is focused on the analysis and synthesis of fixed-thrusters propulsion architectures for AUV in order to achieve a trajectory following task. It provides an analysis of the needed wrench to move the robot throughout all the trajectory following and gives the method to build a compatible thrust configuration matrix (TCM). This fundamental matrix is then used to deduce the propulsion system configuration. In this way, we obtain the minimum number of thrusters, their possible positions and their orientation. In this way we obtain controllable AUVs for the trajectory. The method is first applied to analyze an ill-conditioned AUV that cannot achieve the task, then to analyze and design modified AUVs fit for the task.

2 Dynamic Model of AUV and Propulsion System

2.1 AUV Kinematic and Dynamic Models

To model the AUV, two orthogonal coordinate systems are used: R_0 ($O_0, \mathbf{x}_0, \mathbf{y}_0, \mathbf{z}_0$) is the earth-fixed frame and R_b ($O_b, \mathbf{x}_b, \mathbf{y}_b, \mathbf{z}_b$) is AUV body-fixed. In Fig 1 the AUV is depicted in its body-fixed coordinate system.

The vectors describing the motion of the AUV in 6 DOF are:

$$\boldsymbol{\eta} = (x \ y \ z \ \phi \ \theta \ \psi)^t, \boldsymbol{\nu} = (u \ v \ w \ p \ q \ r)^t$$

Here $\boldsymbol{\eta}$ is the vector of position and orientation in R_0 . The orientation in $\boldsymbol{\eta}$ is defined using an Euler ZYX (ψ, θ, ϕ) convention as described in [6]. $\boldsymbol{\nu}$ is the linear and angular absolute velocity vector in R_b .

To change the AUV velocity vector from one to another coordinate system we use a velocity transformation matrix as given in [6]:

Using this transformation matrix $J(\eta)$, we can obtain the AUV absolute velocity vector expressed in R_0 from its expression in R_b , see [6]:

$$\dot{\boldsymbol{\eta}} = \left. \frac{d\boldsymbol{\eta}}{dt} \right|_{R_0} = \mathbf{J}(\boldsymbol{\eta}) \boldsymbol{\nu} \quad (1)$$

The nonlinear rigid-body dynamic equations of the underwater robot, can be formulated as in [1] and [6]:

$$\mathbf{M}\dot{\boldsymbol{\nu}} + \mathbf{C}\boldsymbol{\nu} + \mathbf{D}\boldsymbol{\nu} + \mathbf{G} = \boldsymbol{\tau} \quad (2)$$

where $\mathbf{M} \in \mathbb{R}^{6 \times 6}$, $\mathbf{C} \in \mathbb{R}^{6 \times 6}$ and $\mathbf{D} \in \mathbb{R}^{6 \times 6}$ are the matrices of mass, Coriolis and centripetal terms, and damping respectively, including added mass terms. \mathbf{G} is the vector of gravitational forces and moments. Lastly, $\boldsymbol{\tau}$ is the wrench of external forces and moments (6 DOF), it accounts for the propulsive wrench generated by the thrusters. $\boldsymbol{\tau}$ is calculated as follows:

$$\boldsymbol{\tau} = \mathbf{B} \mathbf{u} \quad (3)$$

where \mathbf{B} is the thrust control matrix (TCM), which depends on the propulsion system configuration (number, position and orientation of the actuators). \mathbf{u} is the vector of the thrusters forces, i.e., the thrusts.

Added mass effects, drag forces and gravitational/buoyancy efforts are included in matrices of Eqn. (2) as described in Fossen [6] and Antonelli [1] and in our previous works [21].

2.2 Fixed Propulsion System Model

AUVs with this type of propulsion are powered by several thrusters placed along different axis in order to combine their thrust and provide six (or less) actuated DOF to the robot. This architecture uses a multi-directional propulsion based on force combination. Fig. 1 shows the ‘‘RSM’’ AUV which includes 4 thrusters: 2 horizontal thrusters are placed at the rear of the AUV and two vertical ones are centered symmetrically on the sides. This configuration provides actuation over the following DOF: Surge (linear motion along the \mathbf{x}_b -axis), Heave (linear motion along the \mathbf{z}_b -axis), Yaw (rotation along the \mathbf{y}_b -axis) and Roll (rotation along the \mathbf{x}_b -axis). Due to this configuration, 2 DOF are not actuated: Pitch (rotation along \mathbf{y}_b -axis) and Sway (linear motion along \mathbf{y}_b -axis). Roll and Pitch motions are mechanically stabilized thanks to the relative position of the buoyancy and gravity centers. Conversely to the Pitch, the Sway is not controlled and not stabilized, thus free motion on \mathbf{y}_b -axis (drift) is expected to occur.

The thrusters position vectors with regard to R_b are:

$$\mathbf{P}_1 = \begin{bmatrix} P_{1x} \\ P_{1y} \\ P_{1z} \end{bmatrix}, \mathbf{P}_2 = \begin{bmatrix} P_{2x} \\ P_{2y} \\ P_{2z} \end{bmatrix}, \mathbf{P}_3 = \begin{bmatrix} P_{3x} \\ P_{3y} \\ P_{3z} \end{bmatrix}, \mathbf{P}_4 = \begin{bmatrix} P_{4x} \\ P_{4y} \\ P_{4z} \end{bmatrix}$$

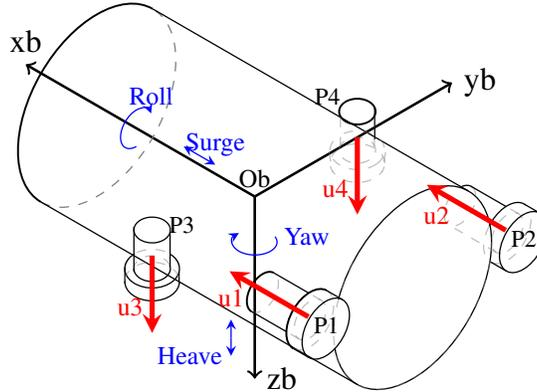


Fig. 1: RSM AUV: 4-fixed thrusters architecture

The RSM AUV thrust control matrix can then be calculated as:

$$\mathbf{B} = \begin{bmatrix} 1 & 1 & 0 & 0 \\ 0 & 0 & 0 & 0 \\ 0 & 0 & 1 & 1 \\ 0 & 0 & -P_{3y} & -P_{4y} \\ P_{1z} & P_{2z} & P_{3x} & P_{4x} \\ -P_{1y} & -P_{2y} & 0 & 0 \end{bmatrix} \quad \text{with } \mathbf{u} = \begin{bmatrix} u_1 \\ u_2 \\ u_3 \\ u_4 \end{bmatrix} \quad (4)$$

where u_1 , u_2 , u_3 and u_4 are the thruster propulsion forces. If the AUV is controllable then B is invertible. In this case, it is possible to express the thrust control vector as: $\mathbf{u} = B^{-1}\boldsymbol{\tau}$, where $\boldsymbol{\tau}$ is the required propulsive wrench.

3 Model-Based Anticipation

To analyze the propulsion system w.r.t. the trajectory, we need to estimate the efforts needed to move the AUV during the trajectory tracking. We use the kinematic and dynamic models to compute the needed (or anticipation) torque $\boldsymbol{\tau}_a$ in order to follow the desired trajectory $\boldsymbol{\eta}_d$. The anticipation method we propose will simply “stick” the AUV on the trajectory such as $\boldsymbol{\eta} \equiv \boldsymbol{\eta}_d$. The corresponding vector $\boldsymbol{\tau}_a$ can be understood as the “nominal control”, steering ideally the AUV on the reference trajectory (See Pino and Delaleau [15] in the design spirit and Hagenmeyer and Delaleau [7] in a control perspective). To proceed, we calculate the inverse kinematic and dynamic models to obtain trajectory-dependent anticipation speed $\boldsymbol{\nu}_a$ and efforts (or wrench) $\boldsymbol{\tau}_a$.

The point O_e is an arbitrary point belonging to the AUV, with which we want to follow the trajectory. We can write the velocity of point O_e in R_b :

$$\boldsymbol{\nu}_e = \underbrace{\begin{bmatrix} 1 & 0 & 0 & 0 & \epsilon_z & -\epsilon_y \\ 0 & 1 & 0 & -\epsilon_z & 0 & \epsilon_x \\ 0 & 0 & 1 & \epsilon_y & -\epsilon_x & 0 \\ 0 & 0 & 0 & 1 & 0 & 0 \\ 0 & 0 & 0 & 0 & 1 & 0 \\ 0 & 0 & 0 & 0 & 0 & 1 \end{bmatrix}}_{\mathbf{T}} \underbrace{\begin{bmatrix} u \\ v \\ w \\ p \\ q \\ r \end{bmatrix}}_{\boldsymbol{\nu}}, \quad \mathbf{r}_e = \begin{bmatrix} \epsilon_x \\ \epsilon_y \\ \epsilon_z \end{bmatrix} = \overrightarrow{O_b O_e}$$

with \mathbf{r}_e the position of point O_e in R_b and \mathbf{T} the transformation matrix of velocity $\boldsymbol{\nu}$ from O_e to O_b . Taking into account preceding equations leads to:

$$\dot{\boldsymbol{\eta}}_e = \mathbf{J}(\boldsymbol{\eta}) \boldsymbol{\nu}_e = \mathbf{J}(\boldsymbol{\eta}) \mathbf{T} \boldsymbol{\nu} \quad (5)$$

This allows us to determine the relation between the velocity at point O_e , namely $\dot{\boldsymbol{\eta}}_e$, and the robot anticipation velocity $\boldsymbol{\nu}_a$ at O_b , expressed in R_b :

$$\boldsymbol{\nu}_a = \mathbf{T}^{-1} \mathbf{J}(\boldsymbol{\eta}_2)^{-1} \dot{\boldsymbol{\eta}}_e \quad (6)$$

Based on the dynamic model of the robot described before (Eq. 2), the following anticipation dynamic law is deduced (in R_b):

$$\boldsymbol{\tau}_a = \mathbf{M} \dot{\boldsymbol{\nu}}_a + (\mathbf{C}(\boldsymbol{\nu}_a) + \mathbf{D}) \boldsymbol{\nu}_a + \mathbf{G} \quad (7)$$

Fig. 2 depicts a pipeline following trajectory and Fig. 3 shows the wrench $\boldsymbol{\tau}_a$ we obtained by the anticipation method on the pipeline trajectory following task, applied on a generic AUV (6 DOF).

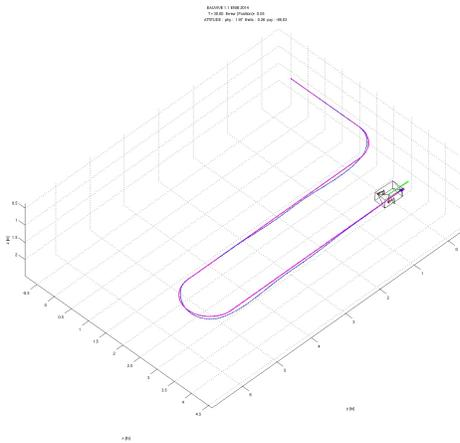


Fig. 2: 3D representation of the trajectory

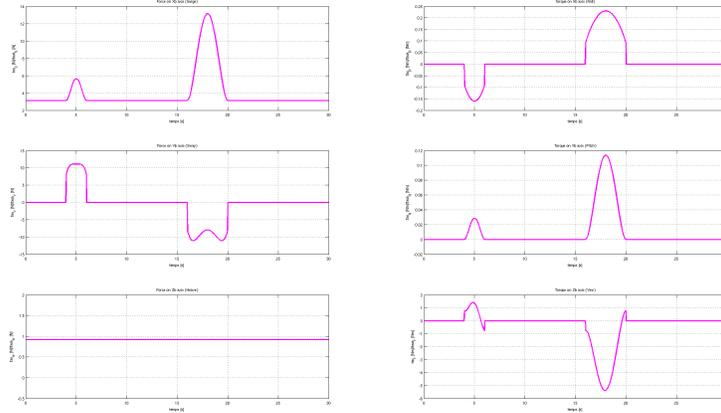


Fig. 3: Efforts in R_b required for the pipeline following task. First column : surge, sway and heave. Second column : roll, pitch and yaw motions.

We can see that for the forces (first column), the propulsion is required on 3 axes, since surge, sway and heave are necessary to maintain the O_e point on the trajectory. Inertia forces demand more efforts during the two turns. Considering the moments (second column), roll and pitch motions do not require any effort outside the turns (the trajectory being planar) while the turns generate small angular accelerations that should be compensated by mechanical stability. Finally, the yaw motion need an important moment during the turns. This can be summarized in the anticipated wrench τ_a by writing: $\tau_a = [* * * 0 0 *]^t$. Note that all stars (*) in a vector stand for independent non zero coefficients.

4 Synthesis of the Propulsion System

All the coordinates, forces and torques are expressed in the AUV frame \mathcal{R}_b . The robot is actuated by K thrusters located in points $P_k = (P_{x,k}, P_{y,k}, P_{z,k})$ (see Fig. 1). The controlled force produced by thruster k is $\vec{F}_k = u_k \vec{f}_k$, where $\|\vec{f}_k\| = 1$ and $|u_k| = \|\vec{F}_k\|$; \vec{f}_k is the *force direction* and u_k is the *thrust* (control variable). Thruster k also produce the torque $\vec{T}_k = \overrightarrow{O_b P_k} \wedge \vec{F}_k = u_k \underbrace{(\overrightarrow{O_b P_k} \wedge \vec{f}_k)}_{\vec{\tau}_k}$

where $\vec{\tau}_k$ is the “normalized” torque.

Each thruster is completely described by its position P_k , its control variable (scalar) u_k and its force direction \vec{f}_k . The *normalized wrench* of thruster k is thus $\vec{\omega}_k = (\vec{f}_k, \vec{\tau}_k)$. The B matrix is constituted by the normalize wrenches: each column of B is precisely the normalized wrench of one thruster.

4.1 Single Thrusters and Basic Configurations

One has seen that each thruster is potentially able to activate several DOF (not independently of course). For the sake of simplicity of the design one seeks for simple situations in which the thrusters could only activate 1 or 2 degree of freedom. In case of 2 DOF, this will be 1 translation and 1 rotation. The 9 configurations are listed and named in Table 1. One sees that a single thruster cannot activate a rotation without activating a translation.

In the sequel, the 3 basic thruster types that activate only translation are generically named as T_{\bullet} and the other 6 ones will be denoted $T_{\bullet\bullet}$.

Table 1: Wrenches associated to some thrusters.

Configuration name	T_x	T_y	T_z	T_{yx}	T_{zx}	T_{xy}	T_{zy}	T_{xz}	T_{yz}
Thruster position	$\begin{bmatrix} P_x \\ 0 \\ 0 \end{bmatrix}$	$\begin{bmatrix} 0 \\ P_y \\ 0 \end{bmatrix}$	$\begin{bmatrix} 0 \\ 0 \\ P_z \end{bmatrix}$	$\begin{bmatrix} 0 \\ P_y \\ P_z \end{bmatrix}$	$\begin{bmatrix} 0 \\ P_y \\ P_z \end{bmatrix}$	$\begin{bmatrix} P_x \\ 0 \\ P_z \end{bmatrix}$	$\begin{bmatrix} P_x \\ 0 \\ P_z \end{bmatrix}$	$\begin{bmatrix} P_x \\ P_y \\ 0 \end{bmatrix}$	$\begin{bmatrix} P_x \\ P_y \\ 0 \end{bmatrix}$
Force direction	$\begin{bmatrix} 1 \\ 0 \\ 0 \end{bmatrix}$	$\begin{bmatrix} 0 \\ 1 \\ 0 \end{bmatrix}$	$\begin{bmatrix} 0 \\ 0 \\ 1 \end{bmatrix}$	$\begin{bmatrix} 0 \\ 1 \\ 0 \end{bmatrix}$	$\begin{bmatrix} 0 \\ 0 \\ 1 \end{bmatrix}$	$\begin{bmatrix} 1 \\ 0 \\ 0 \end{bmatrix}$	$\begin{bmatrix} 0 \\ 0 \\ 1 \end{bmatrix}$	$\begin{bmatrix} 1 \\ 0 \\ 0 \end{bmatrix}$	$\begin{bmatrix} 0 \\ 1 \\ 0 \end{bmatrix}$
Produced Torque	$\begin{bmatrix} 0 \\ 0 \\ 0 \end{bmatrix}$	$\begin{bmatrix} 0 \\ 0 \\ 0 \end{bmatrix}$	$\begin{bmatrix} 0 \\ 0 \\ 0 \end{bmatrix}$	$\begin{bmatrix} -P_z \\ 0 \\ 0 \end{bmatrix}$	$\begin{bmatrix} +P_y \\ 0 \\ 0 \end{bmatrix}$	$\begin{bmatrix} 0 \\ +P_z \\ 0 \end{bmatrix}$	$\begin{bmatrix} 0 \\ -P_x \\ 0 \end{bmatrix}$	$\begin{bmatrix} 0 \\ 0 \\ -P_y \end{bmatrix}$	$\begin{bmatrix} 0 \\ 0 \\ +P_x \end{bmatrix}$

4.2 Thrusters Configuration Design

The aim of this paper is to find a thruster configuration which allows the robot to follow one or several given trajectories. Denotes by $[t_i, t_f]$ the time interval on which the trajectory τ_a is defined: $t \in [t_i, t_f] \rightarrow \tau_a(t) \in \mathbb{R}^6$. Denotes by $\mathcal{J}(\tau_a)$ the vector subspace of \mathbb{R}^6 defined by:

$$\mathcal{J}(\tau_a) = \text{span} \{ \tau_a(t) \mid t \in [t_i, t_f] \}$$

The design procedure consists in finding a family of wrenches $\{\omega_1, \dots, \omega_K\}$ among the T_{\bullet} 's and the $T_{\bullet\bullet}$'s in Table 1 such that:

$$\mathcal{J}(\tau_a) \subset \text{span} \{ \omega_1, \dots, \omega_K \}$$

The the family of thruster $\{\omega_1, \dots, \omega_K\}$ is said to be **minimal** w.r.t. the trajectory τ_a if the two following conditions⁴ are satisfied:

$$\mathcal{J}(\tau_a) \subset \text{span} \{ \omega_1, \dots, \omega_K \} \text{ and } \mathcal{J}(\tau_a) \not\subset \text{span} \{ \omega_1, \dots, \omega_{K-1} \}$$

⁴ The second condition is valid up to a renumbering of the ω_i 's.

Design procedure⁵:

- **Step 1:** Choose as many $T_{\bullet\bullet}$ thrusters as needed rotations⁶.
- **Step 2:** Choose other $T_{\bullet\bullet}$ thrusters in order to cover all/most translations.
- **Step 3:** If needed, choose T_{\bullet} thrusters in order to cover missing translations.

An analysis is done on two already designed AUVs and the design procedure is illustrated to generate a new one that matches the task and is minimal.

4.3 Design Examples

RSM AUV: This existing AUV has 4 thrusters and must follow the pipeline trajectory:

$$\boldsymbol{\tau}_a = \begin{bmatrix} * \\ * \\ * \\ 0 \\ 0 \\ * \end{bmatrix}, \quad \mathbf{B}_{\text{rsm}} = \begin{bmatrix} 1 & 1 & 0 & 0 \\ 0 & 0 & 0 & 0 \\ 0 & 0 & 1 & 1 \\ 0 & 0 & Z_3 & Z_4 \\ 0 & 0 & 0 & 0 \\ -Y_1 & -Y_2 & 0 & 0 \end{bmatrix}, \quad \mathbf{u}_{\text{rsm}} = \begin{bmatrix} u_1 \\ u_2 \\ u_3 \\ u_4 \end{bmatrix}, \quad \boldsymbol{\tau}_{\text{rsm}} = \begin{bmatrix} * \\ 0 \\ * \\ * \\ 0 \\ * \end{bmatrix}$$

One sees that this design corresponds to the choice:

- 2 thrusters T_{xz} (one located at $(X_1 \ Y_1 \ 0)^t$ and the other one at $(X_2 \ Y_2 \ 0)^t$);
- 2 thrusters of type T_{zx} (located in $(0 \ Y_3 \ Z_3)^t$ and $(0 \ Y_4 \ Z_4)^t$).

Finally one has $\mathcal{J}(\boldsymbol{\tau}_a) \not\subset \mathcal{J}(\boldsymbol{\tau}_{\text{rsm}})$ and this AUV cannot perform the task properly. The second star in $\boldsymbol{\tau}_a$ (sway motion) is not matched in $\boldsymbol{\tau}_{\text{rsm}}$ due to the 0. Since this AUV is not suitable for task, we propose to add a fifth thruster to generate the missing surge actuation (see RSM2 below).

RSM2 AUV: The adjunction of a “bow thruster” to RSM gives the RSM2 AUV that has a 5 thrusters and thus can follow the trajectory:

$$\boldsymbol{\tau}_a = \begin{bmatrix} * \\ * \\ * \\ 0 \\ 0 \\ * \end{bmatrix}, \quad \mathbf{B}_{\text{rsm2}} = \begin{bmatrix} 1 & 1 & 0 & 0 & 0 \\ 0 & 0 & 0 & 0 & 1 \\ 0 & 0 & 1 & 1 & 0 \\ 0 & 0 & +Z_3 & Z_4 & 0 \\ 0 & 0 & 0 & 0 & 0 \\ -Y_1 & -Y_2 & 0 & 0 & X_5 \end{bmatrix}, \quad \mathbf{u}_{\text{rsm2}} = \begin{bmatrix} u_1 \\ u_2 \\ u_3 \\ u_4 \\ u_5 \end{bmatrix}, \quad \boldsymbol{\tau}_{\text{rsm2}} = \begin{bmatrix} * \\ * \\ * \\ * \\ 0 \\ * \end{bmatrix}$$

On sees that RSM2 is obtained from RSM by adding one thruster of type T_{yz} located at $(X_5 \ Y_5 \ 0)^t$. Here we have $\mathcal{J}(\boldsymbol{\tau}_a) \subset \mathcal{J}(\boldsymbol{\tau}_{\text{rsm2}})$ and the AUV can achieve the task. However, the solution is not minimal as $\mathcal{J}(\boldsymbol{\tau}_a) \neq \mathcal{J}(\boldsymbol{\tau}_{\text{rsm2}})$. Here, the roll motion can be actuated whilst it is not a required DOF, which makes this configuration non-minimal w.r.t. the task and we will seek a 4-thrusters of the AUV achieving this task (see NEW AUV below).

⁵ The procedure favors the $T_{\bullet\bullet}$ are they are off-centered and more easily implementable than the T_{\bullet} ones.

⁶ Rotation thrusters $T_{\bullet\bullet}$ are chosen first as they generally induce translations.

NEW AUV: One seeks for a 4-DOF AUV able to track $\tau_a = [**00*]$ trajectories. We here apply the design procedure given in previous section:

- **Step 1:** The needed rotation about z_b require either a T_{xz} or a T_{yz} thruster.
- **Step 2:** At this step we choose either T_{xz}, T_{yz} or T_{yz}, T_{xz}
- **Step 3:** In the two cases, z_b is missing we end-up with the choice of T_z .

The 2 obtained configurations are:

$$\{T_{xz}, T_{xz}, T_{yz}, T_z\}, \{T_{yz}, T_{yz}, T_{xz}, T_z\}$$

Any other choice leads to more thrusters. Notice that same symbol appearing twice in the same configuration mean 2 thrusters of the same type at two different locations. In the next section, only the first case of this NEW AUV will be simulated.

5 Simulation and Results

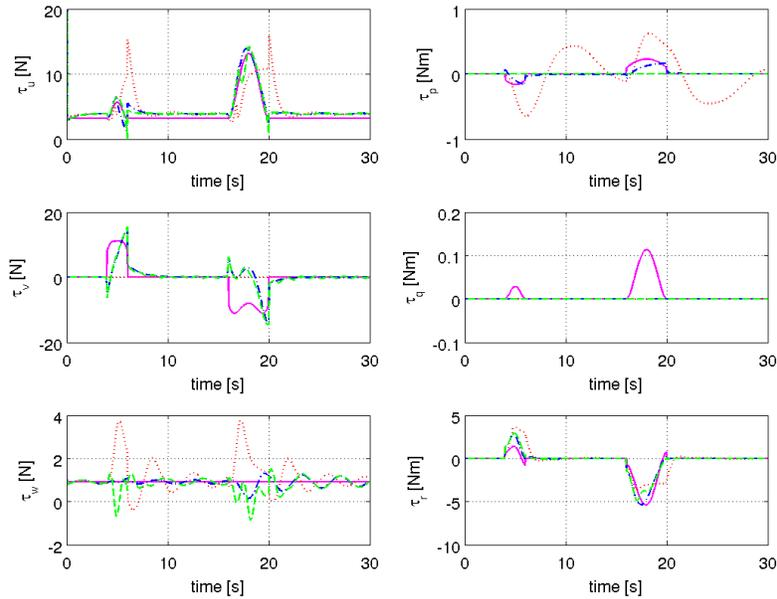


Fig. 4: AUV propulsion efforts : Ref – RSM – – RSM2 .- NEW ..

The studied trajectory is depicted in Fig. 2. The 3 different configurations, namely “RSM”, “RSM2” and “NEW”, are considered and compared. Fig. 4 reports the

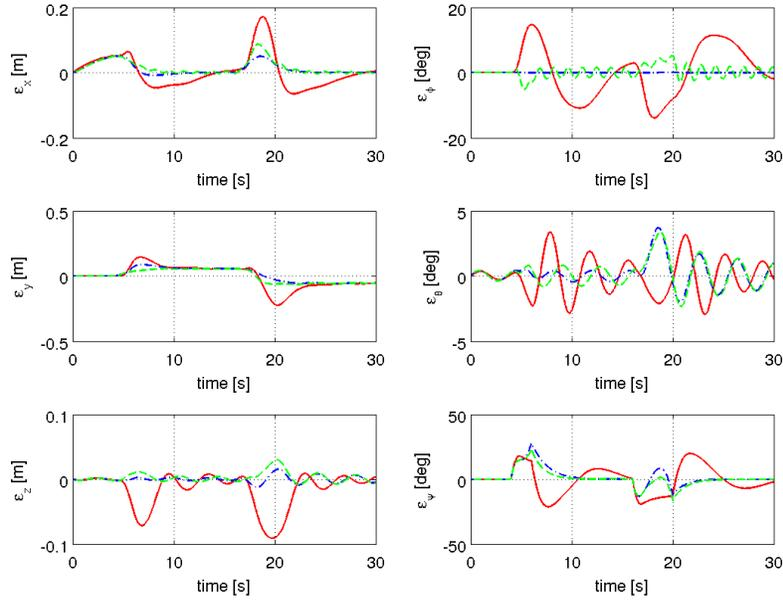


Fig. 5: AUV trajectory errors : RSM – RSM2 .– NEW – –

propulsion efforts whilst Fig. 5 express the position and angular errors w.r.t. the desired reference trajectory. In the simulations, the control of the AUV is achieved by feedback linearization, however, the range of this work extends far beyond this method.

6 Conclusion

The main result of this work is to show that it is possible, knowing the dynamic model of the AUV to build an intrinsically controllable AUV thanks to a specifically designed propulsion system. We showed why some AUVs are unable to achieve a given family of trajectory tasks and how to make it fit to do so. Moreover, we proposed a mathematical and programmable method to build a rational and controllable AUV, using the minimum number of thrusters to perform a trajectory following task. Simulations have been achieved to validate the design. Future works will deal with the generalization to other propulsion modes (not only thrusters) and will improve the control techniques based on nonlinear models. Real word experiments for trajectory following missions will then be done to validate the propulsion synthesis.

Bibliography

- [1] Antonelli G (2006) *Underwater Robots: Motion and Force Control of Vehicle-Manipulator Systems*. Springer-Verlag, New York, NJ
- [2] Cavallo E, Michelini RC, Filaretov VF (2004) Conceptual design of an auv equipped with a three degrees of freedom vectored thruster. *J Intell Robot Syst Theory Appl* 39(4):365–391
- [3] Chocron O, Mangel H (2008) Reconfigurable magnetic-coupling thrusters for agile auvs. In: *IEEE/RSJ Int. Conf. Intell. Robot. Syst.*, Nice, France, pp 3172–3177
- [4] Chocron O, Prieur U, Pino L (2014) A validated feasibility prototype for auv reconfigurable magnetic coupling thruster. *IEEE/ASME Trans Mechatronics* 19(2):642–650
- [5] Chocron O, Vega EP, Benbouzid MEH (2018) Evolutionary dynamic reconfiguration of auvs for underwater maintenance. In: Jaulin Lea (ed) *Marine Robotics and Applications, Ocean Engineering & Oceanography*, vol 10, Springer, Cham, pp 137–178
- [6] Fossen TI (1994) *Guidance and Control of Ocean Vehicles*. Wiley, New York
- [7] Hagenmeyer V, Delaleau E (2003) Exact feedforward linearization based on differential flatness. *International J Control* 76(6):537–556
- [8] Khalil W, Gallot G, Boyer F (2007) Dynamic modeling and simulation of a 3-d serial eel-like robot. *IEEE Trans Syst Man Cybern Part C (Applications Rev)* 37(6):1259–1268
- [9] Kopman V, Cavaliere N, Porfiri M (2012) Masuv-1: A miniature underwater vehicle with multidirectional thrust vectoring for safe animal interactions. *IEEE/ASME Trans Mechatronics* 17(3):563–571
- [10] Le Page YG, Holappa KW, Page L (2000) Hydrodynamics of an autonomous underwater vehicle equipped with a vectored thruster. In: *Ocean. 2000 MTS/IEEE Conf. Exhib. Conf. Proc.*, IEEE, vol 3, pp 2129–2134
- [11] Lin X, Guo S (2012) Development of a spherical underwater robot equipped with multiple vectored water-jet-based thrusters. *J Intell Robot Syst* 67(3-4):307–321
- [12] Nagashima Y, Taguchi N, Ishimatsu T (2006) Development of a compact hybrid underwater vehicle using variable vector propeller. In: *Proc. 23rd Int. Symp. Autom. Robot. Constr.*, pp 66–71
- [13] Nawrot MT (2012) Conceptual design of a thrust-vectoring tailcone for underwater robotics. PhD thesis, Massachusetts Institute of Technology, Cambridge, MA
- [14] Palmer AR (2009) Analysis of the propulsion and manoeuvring characteristics of survey-style auvs and the development of a multi-purpose auv. PhD thesis, School of Engineering Sciences, Faculty of Engineering, Science & Mathematics, University of Southampton, UK

- [15] Pino L, Delaleau E (2006) Flatness-based computer-aided design of mechanical systems. In: Prepr. 13th IFAC Workshop on Control Applications of Optimisation (CAO'06), Cachan, France
- [16] Schultz JA (2009) Autonomous underwater vehicle (AUV) propulsion system analysis and optimization. Master's thesis, Virginia Polytechnic Institute and State University
- [17] Shea D, Williams C, He M, Crocker P, Riggs N, Bachmayer R (2010) Design and testing of the marport SQX-500 twin-pod auv. In: 2010 IEEE/OES Autonomous Underwater Vehicles, pp 1–9
- [18] Sheng L, Dong R, Bing L, Xucheng C (2010) Research on variable direction rotatable axis variable vector propeller of auv in vertical motion. In: Int. Forum Inf. Technol. Appl., IEEE, vol 3, pp 267–270
- [19] Steenson LV, Phillips AB, Rogers E, Furlong ME, Turnock SR (2011) Control of an AUV from thruster actuated hover to control surface actuated flight. Tech. Rep. RTO-MP-AVT-189, NATO
- [20] Tran Nh, Woo MM, Choi Hs, Kim JY (2012) Development of a new underwater disk robot. In: 2012 Ocean. - Yeosu, IEEE, pp 1–9
- [21] Vega EP, Chocron O, Ferreira JV, Benbouzid MEH, Meirelles PS (2015) Evaluation of auv fixed and vectorial propulsion systems with dynamic simulation and non-linear control. In: IECON 2015 - 41st Annu. Conf. IEEE Ind. Electron. Soc., IEEE, pp 944–949
- [22] Vega EP, Chocron O, Benbouzid MEH (2016) A flat design and validated model for auv reconfigurable magnetic coupling thruster. IEEE/ASME Trans Mechatronics pp 2892–2901
- [23] Vestgard K, Hansen R, Jalving B, Pedersen OA (2001) The HUGIN 3000 survey AUV. In: Eleven Int. Offshore and Polar Eng. Conf., Stavanger, Norway, pp 679–684
- [24] Wasylyszyn J (2005) Active control of underwater propulsor using shape memory alloys
- [25] Yu J, Hu Y, Fan R, Wang L, Huo J (2006) Construction and control of biomimetic robotic dolphin. In: Proceedings 2006 IEEE International Conference on Robotics and Automation (ICRA 2006), pp 2311–2316
- [26] Zhou C, Low KH (2012) Design and locomotion control of a biomimetic underwater vehicle with fin propulsion. IEEE/ASME Trans Mechatronics 17(1):25–35